Prilling and characterization of hydrogels and derived porous spheres from chitosan solutions with various organic acids

Imadeddine Lakehal, Alexandra Montembault, Laurent David, Arnaud Perrier, Raphaël Vibert, Laurent Duclaux, Laurence Reinert

Prilling and characterization of hydrogels and derived porous spheres from chitosan solutions with various organic acids

Imadeddine Lakehal[a], Alexandra Montembault[b], Laurent David[b], Arnaud Perrier[c], Raphaël Vibert[c], Laurent Duclaux[a], Laurence Reinert[a]

[a] : Université Savoie Mont Blanc, Laboratoire Chimie Moléculaire et Environnement (LCME), 73000 Chambéry, France
[b] : Université Claude Bernard Lyon 1, Université de Lyon, Laboratoire Ingénierie des Matériaux Polymères (IMP), CNRS UMR 5223, 69622 Villeurbanne, Cedex France
[c] : Synetude SAS, 5 Rue Vaugelas, 73160 Cognin, France

Corresponding author. Tel. :+33 479758122
E-mail Adress: laurence.reinert@univ-smb.fr (L. Reinert).

Keywords: chitosan, hydrogel, rheology, viscosity, prilling, laminar jet breakup

Abstract: This work emphazises the importance of the solubilizing conditions for the elaboration of chitosan hydrogel beads, which were produced using electromagnetic laminar jet breakup technology, resulting in dried porous beads by further freeze-drying. Paramaters such as the acid nature and concentration (acetic, formic, citric, lactic, maleic and malic, 0.1 to 0.5 mol.L^{-1}), the chitosan concentration (2 to 5 wt %) and composition of the gelation bath (NaOH, with or without EtOH) were studied. Viscosity versus strain rate measurements were carried out on chitosan acidic solutions and the viscoelastic behaviour was studied on hydrogels. The solutions exhibiting the highest viscosities led to the stiffest macrohydrogels, as a result of chitosan carboxylate interactions. Specific surface areas of the freeze-dried beads were determined in the range from 12 to 107 $m^2.g^{-1}$. Their internal texture was observed by Scanning Electron Microscopy. Water uptake was also measured for further use in the field of water purification.

1. Introduction

Chitosan (CS) is an aminated linear copolysaccharide of N-acetyl D-glucosamine and D-glucosamine, mainly produced dy deacetylation of chitin. Chitin is itself a by-product of see food industry, composing crustaceans' cuticles and can also be found in insects' cuticles and in fungi cell walls as a non animal source [1,2]. Solid-state heterogeneous N-deacetylation of chitin leads to chitosan of different acetylation degrees (DA), deacetylation pattern (DP) and molecular mass, depending on chitin source and N-deacetylation process [3–5]. Reacetylation of chitosan of low DA can also yield series of polymers of various DAs [6]. During the last decades, the use of CS has been envisioned in many applications, due to its interesting intrinsic physico-chemical and biological

properties. A variety of applications are reported for chitosan such as in pharmaceutical [7], biomedical [8–10], agri-food [11–13], adsorbent for wastewater treatment [14,15], catalyst substrate [16] and in cosmetic fields [17]. Adsorption for wastewater treatment application exploits chitosan's chelating properties towards various metalic cations or atoms [18]. Many authors have demonstrated that the adsorptive properties of CS are better towards divalent cations and especially towards transition metal cations, e.g. Cu(II)[19] or Zn(II) [20], and Ni(II) [21].

The versatility of chitosan makes it shapable in different forms (membranes, tubes, fibers or spheres) [22], and in different physical states (dry forms with different porosities, hydrogels, solutions…) [23,24]. These various forms allow specific uses, especially in the pharmaceutical and wastewater treatment fields. For example, it can be used as adsorbent in appropriate form of cylindrical or spherical shape in waste water treatment fixed bed columns. The commom methods for bead production are solvent evaporation, coacervation [25] and electrospray ionization [26,27]. Recently, new methods have been introduced and applied to overcome the upscaling limitations such as long processing times and the induced high production costs. A laminar jet break-up technology also called "prilling" is one of these techniques. This process allows the formation of uniform, monodispersed size controlled droplets obtained by the vibration breaking-up of a CS acidic solution jet. The produced droplets are collected and further coagulated in a gelling bath into hydrogel beads [28,29].

In the present study, we have designed a production method to obtain significant amounts of CS beads of millimetric size by using the laminar jet breakup process. This method was developed to ensure a fast production and an industrial scale-up possibility. We investigated the rheological properties of both the CS precursor solutions and the hydrogels, as well as the resulting porosity of the dried beads, in order to optimize the beads production method and the adsorption properties. Indeed, the use of prilling process as a production method requires the knowledge and a fine optimization of the CS viscosity [30] and selection of the organic acid used to solubilize chitosan (by varying CS concentration, nature and concentration of the acid, etc…). In a second step, the mecanical and textural properties of the obtained hydrogels and the resulting dried beads have been finely characterized.

The hydrogel materials produced from CS are known to have relatively low mechanical properties and their dried forms are usually mechanically fragile, so chemical modifications such as grafting or crosslinking are usually needed to modify the structure and enhance their mechanical properties [31]. Thus, much current researches are focused on modifying CS. However, in the present study raw CS was used without chemical modification to take advantage of the "general recognized as safe" property of chitosan. Indeed, raw chitosan can be digested by enzymes found in intestinal tract of

animals and is then converted to N-acetylglucosamine [32]. It is also used as dietary supplement as a cholesterol-lowering agent since it partially trapps dietary fats, thus limiting their absorption by the digestive system [33,34].

In the present study, the CS solution parameters such as acid nature and the CS concentration, were varied in order to better understand their effect on the mechanical strength and the textural properties of the initial and the freeze-dried hydrogels prepared through laminar jet breakup.

2. Materials and methods

2.1 Solution and beads preparation

Chitosan from shrimp shells was purchased from Mahtani Chitosan PVT. Ltd., India (batch type 342). The average Acetylation Degree (DA) was close to 11% as determined according to the Hirai method [35] from liquid state ^{1}H-NMR on a Brucker Avance III 400MHz at 25°C. The mass average molar masses M_W and M_n were measured by Size Exclusion Chromatography (SEC) (2500 and 6000 PW TSK gel columns from Tosoh) coupled online with a differential refractometer (Wyatt Optilab T-rEx) and a multi angle light scattering detector (Wyatt HELEOS) operating at λ = 664.0nm [36]. A degassed 0.2 mol.L^{-1} acetic acid/0.15 mol.L^{-1} ammonium acetate buffer (pH = 4.5) was used as eluent at a flow rate of 0.5 mL.min^{-1}. Refractive index increments (dn/dc = 0.187 mL.g^{-1}) were determined from a previous calibration curve [37]. The molar masses were determined as M_w = 175000 +/- 15000 g.mol^{-1} and M_n = 77430 +/- 6000 g.mol^{-1}.

All organic acids were purchased from Sigma Aldrich and were of analytical grade. CS and other reagents were all used without further purification.

Different acid aqueous solutions of chitosan were prepared varying the acid nature (formic (FA), acetic (AA), lactic (LA), malic (MA), maleic (MeA) and citric (CA)), by dissolution of CS at a concentration (labeled Cp) ranging from 2 to 5% (w/w) by means of adding the acid at different concentrations (0.1 to 0.5 mol.L^{-1}). The solutions were mechanically stirred for 24h and then filtered on 200µm stainless steel filter mesh prior to proceed to the beads production.

The prilling device (**Fig. 1**) was designed by SYNETUDE, (Cognin, France). The chitosan solution (0.5 to 1.5 L) was placed in a pressure vessel with a capacity of 2 L. By application of an air pressure in the range from 0.5 to 3 bars depending on the viscosity of the solution, this latter passed through a vibrating nozzle connected to an electromagnetic vibrator controlled in frequency and amplitude by imposing a sine wave with a low frequency generator (LFG). The jet size could be monitored by the diameter size of the nozzle mounted on the prilling head. Prior to any vibration application, a laminar jet of the CS solution was obtained by varying the air pressure to adjust the jet

velocity. The obtained laminar jet was then cut into regular droplets (thanks to the surface tension) by imposing vibrations which wavelengths are longer than the jet girth diameter. The applied frequencies delivered by the LFG depended on the viscosity of the solutions and varied from 200 to 800 Hz. A LED strobe light settled to the same frequency as the nozzle vibration allowed the visual observation of the droplets jet. These droplets fell into a gelation bath placed several centimeters (~ 10 to 30 cm) below the nozzle, to a position where spheres were formed. Gelation baths composed of 10% (w/w) (*i.e.* 2.5 mol.L^{-1}) sodium hydroxide aqueous solutions [38] or 10% (w/w) sodium hydroxide / 50% (w/w) ethanol (EtOH) hydroalcoholic solutions were used. The most important conditions required for bead formation were the jet velocity (to get a laminar jet and hence a reproducible process) and the frequency at which uniform droplets were obtained [39].

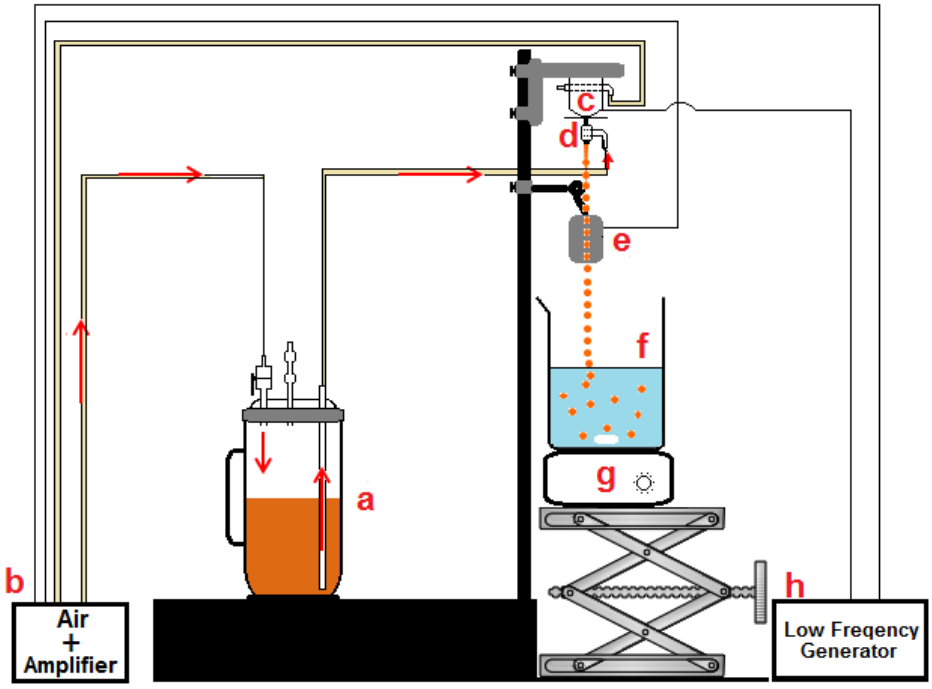

Fig. 1. Schematic drawing of the lab-scale prilling process unit. **a**: pressure vessel containing the chitosan solution, **b**: air setup control, **c**: electromagnetic shaker, **d**: prilling head & nozzle, **e**: strobe light, **f**: gelation bath, **g**: magnetic stirrer, **h**: low frequency generator. Pressure was ranging from 0.5 to 3 bars, frequency from 250 to 800 Hz. Gelation bath was stirred at 250 rpm.

Once produced, the CS solution droplets were neutralized in the gelation bath yielding to spherical millimeter-size hydrogels which were then collected and washed extensively in distilled water until neutrality. The obtained hydrogels produced in a gelation bath composed of 10% sodium hydroxide aqueous solutions were further stored in distilled water. Those produced in gelation bath composed of 10% sodium hydroxide and 50% EtOH were further stored in 50/50 (w/w) mixture of EtOH and water.

The collected hydrogel beads (*i.e.* the "prills") have been lyophilized instead of air dried to avoid the complete collapse of the gel structure (*i.e.* formation of xerogels) by the capillary compression during water evaporation [40]. For the lyophilization, the prills were poured in polypropylene beakers which were immersed and freezed in liquid nitrogen so that prills and liquid nitrogen were not in direct contact. A direct contact between the liquid nitrogen and the hydrogels damages the hydrogels' surface and induces the hydrogel collapse. Small volumes (30mL) were introduced in each beaker to ensure a fast freezing to the prill center as a slower freezing leads to bigger ice crystals and then to a coarser structure. Finally the freezed hydrogels were vaccum dried at 0.024 mbar and -80°C for 3 days.

2.2 Characterization of chitosan solutions, chitosan hydrogels and lyophilized beads

The rheological behavior of the different chitosan solutions was studied using an AR 2000EX TA instrument rheometer with a cone-plate geometry (Aluminum, 4°, 25mm) with a gap of 116 microns. The shear rates were ranged from 0.1 to 1000 s^{-1}. The Newtonian viscosity of the solutions is given by the plateau at low shear rates. The temperature was set to 20°C or 50°C according to the viscosity to be measured. All measurements were performed in triplicate and the average Newtonian viscosity was determined, with a standard deviation < 5%.

The viscoelastic properties of the hydrogels were determined by rheological studies with an ARES TA instrument using a plate-plate geometry of 25 mm diameter. The working gap between the plates was in the range 2-5 mm. As the bead morphology is not adapted for this rheological characterization with such an apparatus, hydrogels in the form of cylindrical pellets of 25 mm diameter and 3 to 5 mm thickness and prepared in the same physico-chemical conditions than the beads were characterized in dynamic mode (same solutions, same coagulation baths, but geometrically different). An oscillatory strain with amplitude of 1% was applied to the sample and the resulting oscillatory stress was measured to deduce the complex modulus. Again, the measurements were performed in triplicate and the average moduli were calculated, the standard deviation was <5%.

Specific surface areas (S_{BET}) of the lyophilized beads were calculated from nitrogen adsorption isotherms at 77K using a Micromeritics ASAP 2020 sorptometer and standard BET (Brunauer-Emmet-Teller) equation within the relative pressure range of 0.05 to 0.35 [41]. Samples were degassed under vacuum (10^{-3} mbar) at 80°C for 24h before measurements. Pore size distributions were calculated from the obtained isotherms applying Barret Joyner and Halenda (BJH) method [42] and assuming a model of cylindrical pores.

The morphology of the lyophilized samples was observed by Scanning Electron Microscopy (SEM) using a LEO stereoscan 440 microscope. To observe the internal porosity, the beads were cut in the middle, avoiding flattening the internal pores.

3. Results and discussion

3.1 Rheological behavior of chitosan solutions and hydrogels

3.1.1 Effect of the concentration of chitosan and the acid nature on the rheological behavior of chitosan solutions

Fig. 1, 2 and **3** display the viscosity measurements of different CS solutions and also illustrate the modelling of the viscosity measurements using the Cross model ($R^2 > 0.98$) according to equation (1).

$$\eta = \frac{\eta_0}{(1+\dot{\gamma}/\dot{\gamma}_c)^p} \qquad \text{(eq. 1)}$$

Where η (Pa.s) is the dynamic viscosity, η_0 (Pa.s) is the Newtonian viscosity at low shear rates, $\dot{\gamma}$ (s^{-1}) is the shear rate, $\dot{\gamma}_c$ (s^{-1}) is the critical shear rate at which the sample starts to behave like a shear-thinning material, and *p* is a dimensionless parameter related to the slope of the power-law region [43]. The resulting values of the different parameters from the fitting to the Cross model are shown in **Tables 1** and **2** as a function of the acid concentration, CS concentration and the nature of the acid respectively.

The effect of concentration of the acid on the viscosity was studied using 3 concentrations of chitosan (2%, 2.5% and 3.5% (w/w)) each at 2 concentrations of acid: 0.5 $mol.L^{-1}$ and a lower amount corresponding to stoichiometric quantity of acid to the number of amine groups (representing 0.11 $mol.L^{-1}$ for 2% of CS, 0.14 $mol.L^{-1}$ for 2.5% of CS and 0.20 $mol.L^{-1}$ for 3.5% of CS).

Parameters influencing the viscosity of the solutions are the acid concentration (**Fig. 2**), CS concentration (**Fig. 3**) and the nature of the acid used for the solubilization (**Fig. 4**). All the solutions displayed a Newtonian plateau at low shear rates and then a shear-thinning behavior from a critical shear rate $\dot{\gamma}_c$ except for 3.5% of CS using stoichiometric quantity of acid (**Fig. 2**). The Cross model did not fit perfectly this latter at the studied shear rates and the value of Newtonian viscosity is hence an approximate value: the viscosity did not scale clearly as $\eta \sim 1/\dot{\gamma}$ which is the signature of a soft gel state, but the observed behavior was intermediate between a solution and a gel. Increasing acid concentrations lead to decreased dynamic viscosities for the 3 samples. The increase in acid concentration is known to lead to lower pH values and higher ionic strengths and hence lower dynamic viscosities [44]. This difference is even more noticeable when increasing chitosan concentration from 2 to 2.5 and 3.5%. The critical shear rate decreases when decreasing acid concentration and hence

increasing the Newtonian viscosity. Since there is less acid, the chains are less screened and are in an extended conformation, which leads to rheofluidifying behavior at lower values of shear rates. This phenomenon is clearly noticeable comparing the samples 2.5-AA-SQ and 2.5-AA-0.5.

Fig. 3 displays the impact of chitosan concentration at a constant acetic acid concentration of (0.5 mol.L^{-1}. Again, all solutions displayed a Newtonian plateau at low shear rates and then a shear-thinning behavior, except for of chitosan concentrations Cp=4.5% and 5%: these samples do not exhibit a Newtonian plateau in the studied frequency range. Numerically, the Cross model modeling was difficult and thus the values of Newtonian viscosity for these two samples should be taken as with some caution. The Newtonian viscosity strongly increased with chitosan concentration C_p. (**see Table 1**). This can be classically explained by more entanglements between the CS chains, restricting the degree of freedom of the chains at high polymer concentration [45,46].

The evolution of the critical shear rate of the samples prepared with different chitosan concentration is shown in **Fig. 3** and **Table 1**. The critical shear rate is greatly reduced when increasing the CS concentration. The average value of the parameter *p* (0.56) is consistent with the one found by Calero *et al*. [43] but lower than that of Halimi *et al*. [47] who used a combination of Couette rheometry and capillary rheometry. Thus the value obtained from our data should be interpreted with care and should be confirmed by extended flow diagram using capillary rheometry measurements at higher shear rates where the slope of the curve is defined in a larger shear rate range.

The effect of the nature of the acids on the viscosity of CS solutions was studied at a constant molar concentration (0.5mol.L^{-1}) and a constant CS concentration (4% (w/w)) at 20°C (**Fig. 4**). The molecular weight of chitosan after dissolution in the different acids was determined by SEC to ensure that the different viscosities were not impacted by a decrease in the molecular weight due to acidic hydrolysis of the glycosidic linkages. In the present study, no effect was observed and the average molecular masses remained unchanged (M_w = 175000 +/-15000 g.mol^{-1}). Mono-(acetic, formic and lactic), di-(malic and maleic) and tri-(citric) acids have been tested. The pKa of the acids used [48] for the solubilization and the pH of the CS solutions after 24h of stirring are reported in **Table 3**. The observed pH ranged from 4 to 1.4 according to the nature of carboxylic acid used. In these conditions, the dissociation degree of chitosan is close to 0 *i.e*. the amine groups of chitosan are totally protonated. Thus, for a degree of acetylation of DA=11% and ionic strength above 0.1 mol.L^{-1}, the apparent pK_a of chitosan base is close to 6.3 [6,49]. Such hypothesis enabled us to estimate of pH (using CurtiPlot software [50]). Calculations systematically led to pH values significantly higher than the experimental ones. Practically, such calculated results are not impacted by the exact value of the pK_a of chitosan used (when the pKa of chitosan is chosen above 5). Such free protons in excess in the

solution should originate from a higher dissociation of the acids, and thus from a change in their pK_a in comparison with their standard values. *n*-carboxylic acids are known to interact with chitosan through ionic and H-bonding/hydrophobic interactions in aqueous solutions [51]. The formation of complexes involving proton– chitosan– carboxylate species was also evidenced showing a quantitative sequestering capacity of chitosan towards the carboxylates [52]. If such sequestration occurs between carboxylate and chitosan, the pKa of the corresponding acid could be lowered to favor a proton release and thus the decrease of pH. The impact of such complexation is thus to increase the ionic force, but could also act on the density of charge of the polymer (although for long chain acids, steric hindrances could yield chain rigidity) and thus should decrease the viscosity of acidic chitosan solutions. The dissociation degree (α) of each monoacid in the experiment conditions and the ionic strength (*I*) have been calculated at the measured pH thanks to equation 2 and equation 3 respectively [44] and the resulting values are presented in **Table 3.** The first dissociation pKa_1 values were used for the calculations of ionic strengths for all acidic solutions since pH revealed all acids were in their associated form.

$$\alpha = \frac{[conjugated\ base]}{[conjugated\ base]+[acid]} = \frac{10^{-pKa}}{10^{-pKa}+10^{-pH}} \qquad \text{(eq. 2)}$$

$$I = \frac{1}{2}\sum_1^n Z_i^2 c_0\ \alpha_i + 10^{-pH} \qquad \text{(eq. 3)}$$

The same equations could be used for polyacids (malic, maleic and citric), neglecting the second and third dissociations occurring at much higher pH.

From **Fig. 4** and Cross model modeling (**Table 2**), it could be noticed that the minimum Newtonian viscosities were obtained when using maleic acid which is the more dissociated acid (α=0.42) and hence exhibits the higher ionic strength (I=0.1 $mol.L^{-1}$). On the opposite, acetic, formic, lactic and malic acids, which have higher pKas, displayed low dissociation degrees and also led to the solutions with the lowest pH after solubilization, the lowest ionic strengths, and the highest viscosities (see **Table 2**). Hamdine *et al*. have suggested that molecular parameters of the acids (local electronegativity and molar volume of the carboxylate) relate to the value of viscosity [44]). In addition to 2 hydroxyl groups favoring H-bonding, citric carboxylate have the highest molecular volume and apparently binds efficiently to chitosan chains, which induces chain neutralization and a reduction of the electrostatic contribution of the chain persistence length, reducing the viscosity.

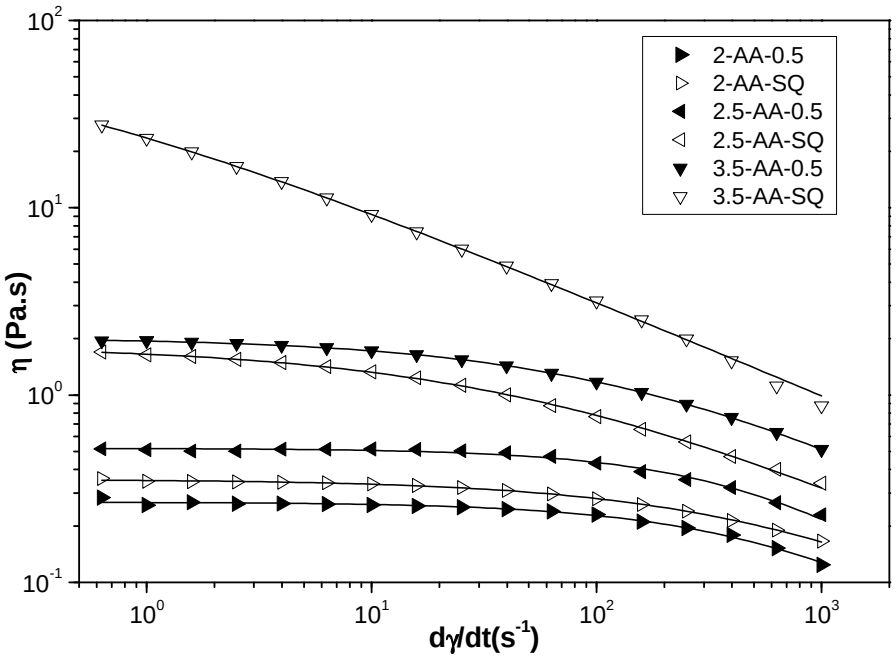

Fig. 2 Viscosities of chitosan solutions prepared with different concentrations of acetic acid and chitosan. Continuous lines illustrate the modeling with Cross equation (equation 1). The samples are labeled X-Acid Acronym-Y, where X is the % (w/w) concentration of chitosan and Y is the molarity of acetic acid. SQ=Stoichiometric Quantity of acid to the number of amine groups (= 0.11 mol.L^{-1} for 2% of CS, 0.14 mol.L^{-1} for 2.5% of CS and 0.2 mol.L^{-1} for 3.5% of CS).

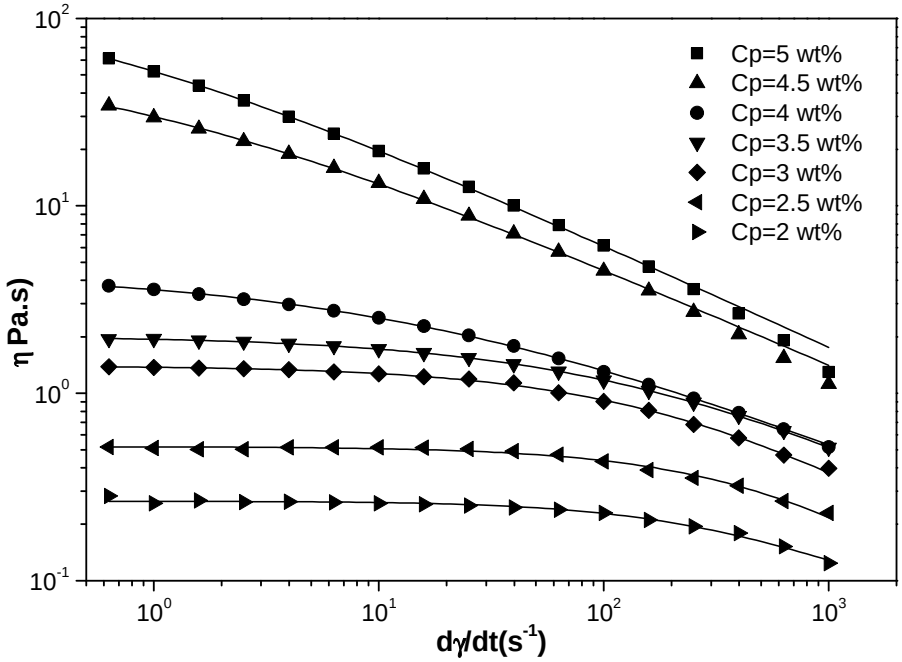

Fig. 3. Dynamic viscosities of chitosan solutions prepared with different concentrations of chitosan (Cp=2, 2.5, 3, 3.5, 4, 4.5 and 5% w/w) in 0.5 mol.L^{-1} acetic acid. For Cp<4.5%, the Newtonian viscosity is extrapolated from the plateau at low shear rates. Continuous lines illustrate data the modelling with Cross equation (equation 1).

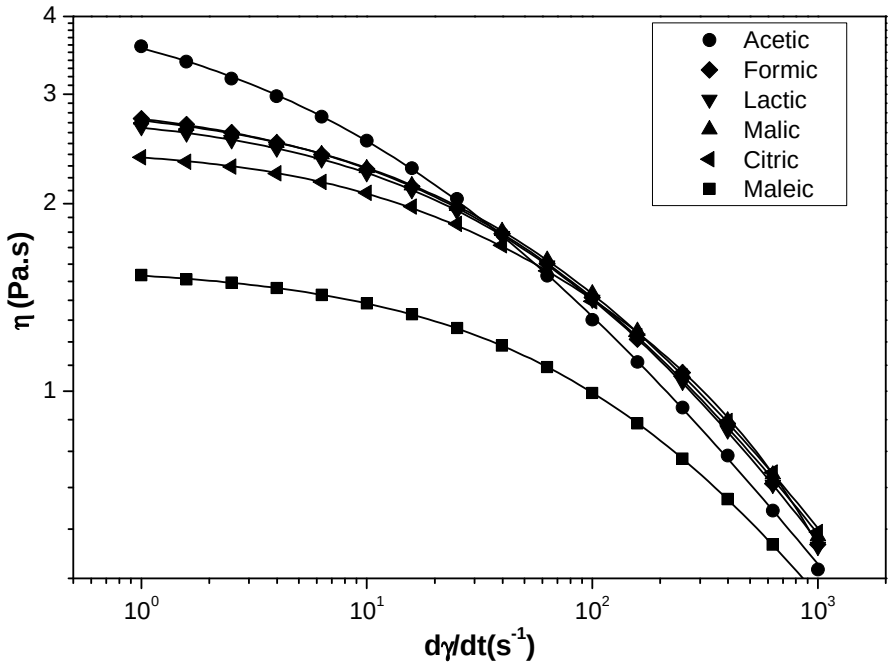

Fig. 4. Viscosities of chitosan solutions prepared in acidic aqueous solutions with different acids (acetic, formic, lactic, malic, maleic and citric) at 0.5 mol.L^{-1} and at the same chitosan concentration (4% w/w). Continuous lines illustrate the Cross model data modeling (equation 1).

Table 1. Parameters for flow curves modeling the Cross model for the chitosan acetate solutions with different acetic acid and chitosan concentrations. T = 20°C. SQ=Stoichiometric Quantity of acid to the number of amine groups (= 0.11 mol.L^{-1} for 2% of CS, 0.14 mol.L^{-1} for 2.5% of CS and 0.2 mol.L^{-1} for 3.5% of CS)

Sample	η_0 (Pa.s)	$\dot{\gamma}_c$ (s^{-1})	p
2-AA-0.5	0.27	258.0	0.46
2-AA-SQ	0.35	85.6	0.64
2.5-AA-0.5	0.48	188.9	0.53
2.5-AA-SQ	1.65	10.7	0.54
3-AA-0.5	1.40	64.9	0.71
3.5-AA-0.5	2.22	30.9	0.62
3.5-AA-SQ	34.4	$<10^{-10}$	0.51
4-AA-0.5	3.72	4.2	0.50
4.5-AA-0.5	66.1	$<10^{-9}$	0.53
5-AA-0.5	148.5	$<10^{-20}$	0.55

The standard deviation of the mean for at least 3 replicates for η_0 is <5%.
The standard deviation of the mean for at least 3 replicates for $\dot{\gamma}_c$ is <5%.
The accuracy for the determination of *p* is close to +/-0.15

Table 2. Parameters for flow curves modeling the Cross model for chitosan solutions (Cp=4% w/w) solubilized in acid aqueous solutions with different acids at the same concentration of 0.5 mol.L^{-1} (acetic, formic, lactic, malic, maleic, and citric). T = 20°C.

	Acetic	Formic	Lactic	Malic	Maleic	Citric
η_0 (Pa.s)	3.72	2.92	2.81	2.90	1.59	2.48
$\dot{\gamma}_c$ (s^{-1})	5.1	16.4	19.9	17.7	36.7	28.2
p	0.50	0.58	0.59	0.58	0.60	0.61

Table 3. pKa of the acids used (0.5 mol.L^{-1}) for the solubilization of chitosan and pH of the CS solutions (Cp=4%) after 24h magnetic stirring. Dissociation degrees of the acids and calculated ionic strength

Acid	pKa_1	pKa_2	pKa_3	pH after 24h (+/- 0.1)	Calculated pH	α	I (mol.L^{-1})
Acetic	4.765			4.0	4.50	0.15	0.037
Formic	3.74			2.9	3.50	0.13	0.033
Lactic	3.86			3.3	3.61	0.22	0.054
Malic	3.40	5.1		2.7	3.18	0.15	0.039
Maleic	1.89	6.23		1.8	1.74	0.42	0.114
Citric	3.13	4.76	6.40	2.3	2.85	0.12	0.034

3.1.2 Viscoelastic properties of hydrogels

Hydrogels were prepared from different CS acidic solutions followed by neutralization in 2.5 mol.L^{-1} NaOH and washing. The viscoelastic properties of the hydrogels were investigated by measuring their dynamic storage (G', Pa) and loss (G'', Pa) shear moduli versus angular frequency, in the range from 100 to 0.05 rad.s^{-1}. The loss factors (equation 4), independent of geometrical factors, and were calculated for all the samples at the studied frequencies.

$$Tan\,\delta = \frac{G''}{G'} \qquad \text{(eq. 4)}$$

All samples displayed a typical viscoelastic behavior characteristic of physical gels with G' > G''. The values of G', G" and Tan(δ) were all almost frequency independent in the investigated angular frequency range, which is characteristic of strong gels. The storage moduli of hydrogels (**Fig. 5** and **6**) are correlated with the values of the Newtonian viscosities of their mother solutions as shown in **Fig. 8**. Indeed, solution with a high Newtonian viscosity generally yielded hydrogels with a high storage modulus. As a result, the storage modulus also depended on the nature of the acid used to solubilize chitosan even if the most impacting parameter was the chitosan concentration. Accordingly, the solution prepared in acetic acid gives the hydrogel having the highest storage modulus (**Fig. 6**), while those prepared in citric and maleic acids yield to hydrogels with the weakest storage moduli as for the Newtonian viscosity. Such correlated behaviour of the solutions and gels prepared in maleic and citric acids are well noticeable in **Fig. 8**. Similar relations between viscosity of the solutions and modulus of the gels were also reached for gels obtained from different neutralization routes and different chitosan concentrations [53].

The hydrogel storage modulus depends on the density of physical junctions in the polymer network. In addition to H-bonds and hydrophobic interactions, entanglements contribute to the formation of inter-chain junctions within the hydrogel. Strong entanglement density is found in highly charged polyelectrolyte solutions, and the hydrogels resulting from these solutions may also exhibit high viscoelastic moduli if the neutralization conditions permitted to preserve the entanglements entrapped in the hydrogel, i.e. if neutralization is fast [54]. Indeed, low DA chitosan chains in solution occupy a large volume due to intra-chain repulsive interactions. Since the modulus of the gels is impacted by entrapped entanglements after neutralization, a decrease in the initial entanglement density in the solution is expected to yield softer gels [54]. This may occur when the ionic force in the initial solution is high (because electrostatic interactions are screened and thus the entanglement density decreases) or is the chains are partly neutralized due to carboxylate/chitosan/proton complexes. The ionic force in chitosan citrate and chitosan maleate solutions is larger than the other acetic and formic acid solution. In addition, the nature of carboxylic acids also impacts the viscosity of the solutions through carboxylate/chitosan interactions. In the hydrogels however, such interactions should be largely impacted by neutralization of chitosan chains with the vanishing contribution electrostatic attractions, but polyacids (citric and maleic) with high pK_as could preserve their hydroxyl groups for hydrogen bonding up to high pH and may also impact crystallization of the hydrogels. Such crystallization is likely to occur after neutralization when the DA of chitosan is below 15% [55]. Tanigawa *et al*. have shown that interactions between citric acid and chitosan and between acetic acid and chitosan lead to different crystallinity in solid form, resulting from different interactions between carboxylates and chitosan in the precursor solutions [56]. These combined effects could contribute to the low values of the storage modulus for the hydrogels formed from chitosan citrate and chitosan maleate solutions. Furuike *et al*. have suggested that the high hydrated state of the chitosan hydrogels contributes to spread the intermolecular distance between chitosan chains and hence the carboxylates could easily interact with CS macromolecules [57]. The molecular volume of each carboxylate probably plays a major role in the interchain interactions of such hydrated materials, since citrate and maleate having bigger molecular volumes lead to the lowest storage moduli.

The composition of the gelation bath also impacted the viscoelastic properties of the hydrogels. Using EtOH in the gelation bath and in the storage solution led to higher values of the storage moduli, but only for the samples prepared in acetic and formic acids (**Fig. 7**). Adding ethanol in the solvent changes the dissociation constants of the acids, the ionic force, and also plays a role in the establishment of competitive interactions between carboxylate, chitosan and ethanol. In practice, using citric acid to dissolve the chitosan, EtOH/water based gelation yielded lower values of storage modulus in comparison with aqueous solvent. Since water is needed for the crystallization of the

hydrated form of chitosan allomorph, EtOH/water gelation usually induces a mixed and ill-defined crystallinity with both hydrated and anhydrous forms [9]. Thus apparently, gelation and crystallization were significantly hindered in presence of EtOH using citric acid.

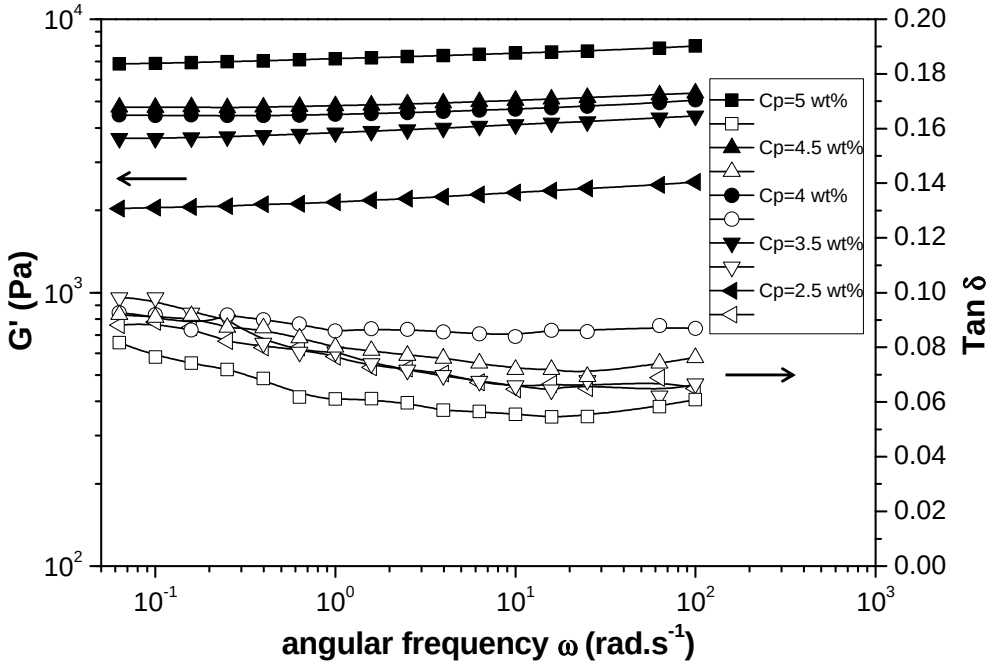

Fig. 5. Storage (full symbols) and loss (empty symbols) moduli of chitosan hydrogels prepared from chitosan solutions at different concentrations, Cp ranging from 2.5 to 5% w/w in 0.5 mol.L^{-1}acetic acid.

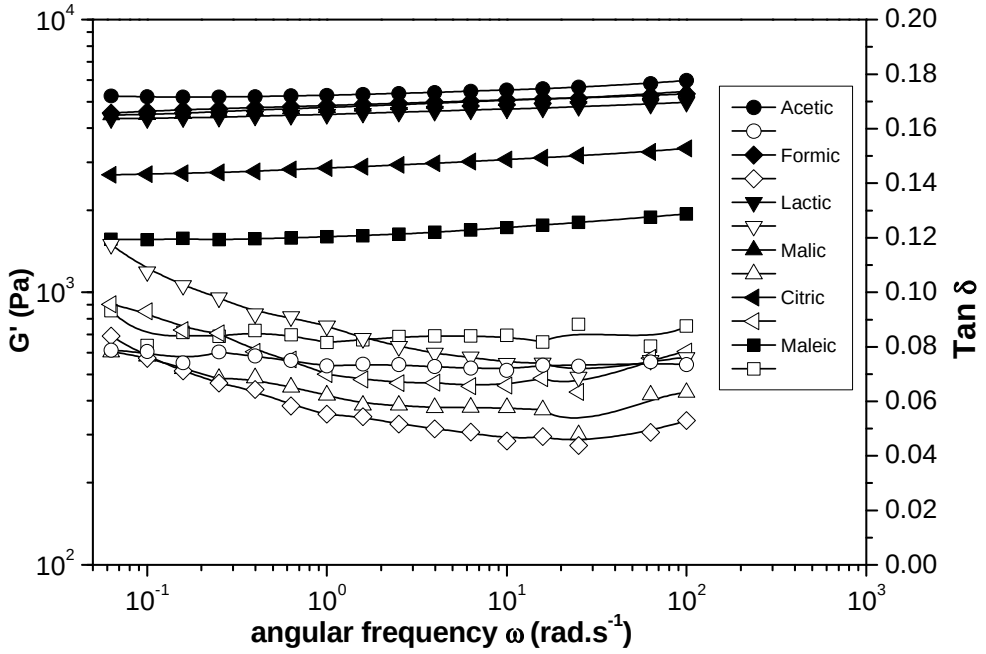

Fig. 6. Storage (full symbols) and loss (empty symbols) shear moduli of hydrogels prepared from chitosan solutions at Cp= 4% w/w solubilized in different acids (acetic, formic, malic, lactic, citric and maleic) at 0.5 mol.L^{-1}.

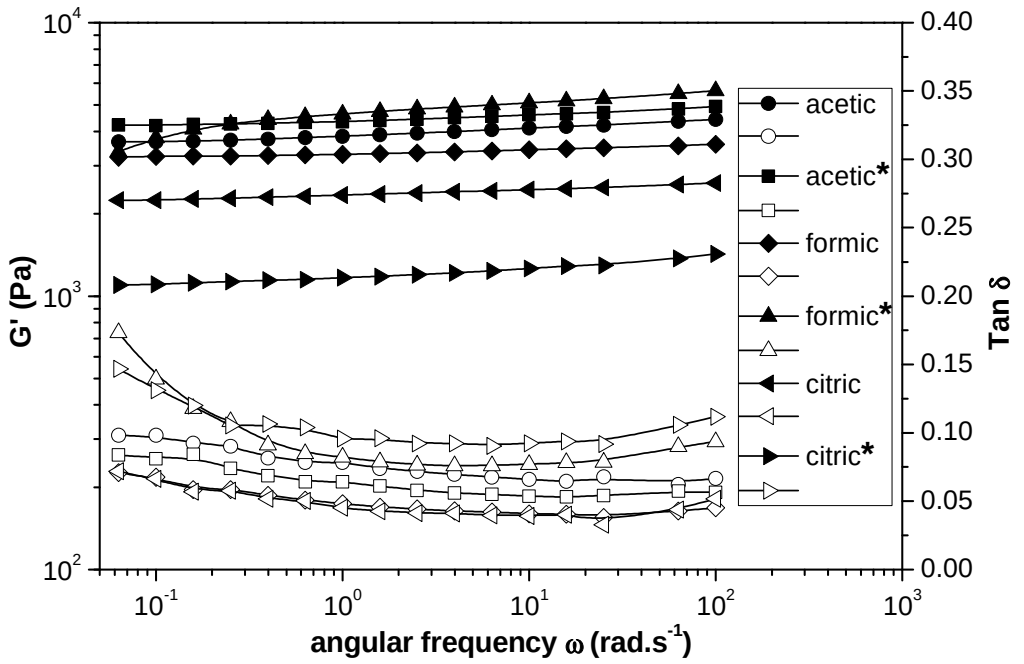

Fig. 7. Storage (full symbols) and loss (empty symbols) moduli of hydrogels prepared from chitosan solutions at Cp=3.5% w/w solubilized in 3 different acids (acetic, formic and citric) at 0.5 mol.L^{-1}. Samples labeled with (*) were prepared through the use of ethanol in the gelling bath and the storage solution (50/50 w/w).

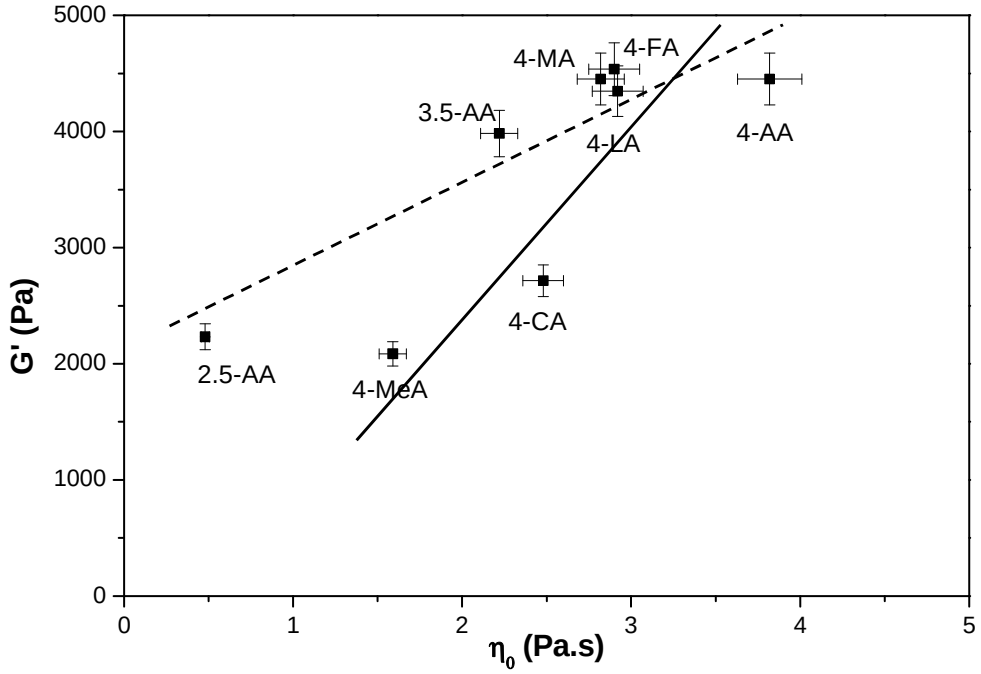

Fig. 8. Correlation between the Newtonian viscosities and the storage moduli of the chitosan solutions and hydrogels prepared from solutions of 2.5%, 3.5% and 4% of chitosan solubilized in acetic acid and 4% of chitosan solubilized in the different acids. Nomenclature:X-Acid type, where X is the % (w/w) concentration of chitosan. Interrupted line and straight line represent least square lines for chitosane concentration correlation and acid correlation respectively.

3.1.3 Viscosity required for the prilling process

The suitable average Newtonian viscosity for a further use of the prepared solutions in the laminar jet break-up process was empirically determined to range between 1 and 3 Pa.s. This value is required to obtain solution flow through a nozzle of 1mm diameter to form a laminar jet at a pressure lower than 3 bars. At higher viscosities, a laminar jet flow could hardly be obtained in the studied conditions of prilling. Below 1 Pa.s the drops were obtained, but they were deformed at their impact at the surface of the gelation bath yielding distorted hydrogel spheres with poor mechanical strength. Chitosan concentration Cp ranging from 3.5% to 4% were the best compromises to get an easy-to-use solution for prilling and to obtain hydrogels with storage moduli suitable for easy handling. In order to use solutions of higher CS content (Cp>4%w/w), the temperature was increased up to 50°C. This allowed to decrease the Newtonian viscosity making possible the use of high CS content solutions through the prilling process unit.

The shear rate $\dot{\gamma}_n$ inside the nozzle could be estimated knowing the solution volumetric flow rate Q ($m^3.s^{-1}$) and the nozzle radius *R* (m) using equation 5. This value of the apparent shear rate allows determining the viscosity of the solution passing through the nozzle, using the flow diagrams determined in **Fig. 2** to **4**.

$$\dot{\gamma}_n = \frac{4Q}{\pi R^3} \qquad \text{(eq. 5)}$$

The shear rate inside the nozzle was comprised between 500 and 1100 s^{-1} for the studied solutions which corresponded to viscosities inside the nozzle lower than 2 Pa.s for all the “prillable” formulations.

3.2 Dried beads characterization

3.2.1 Specific surface area and apparent pore size distribution

The N_2 adsorption-desorption isotherms of lyophilized hydrogel beads prepared by prilling highlight the structural effect of processing parameters such as chitosan concentration, EtOH addition in the gelling bath and the nature of the acid used for solubilization, by the evaluation of the specific surface areas. All the lyophilized hydrogels displayed a type IV profile with a hysteresis between the adsorption and desorption curves, typical of the presence of mesopores. The use of different acids for CS dissolution leads to different specific surface areas (**Table 4**). For the same gelation conditions (Cp = 4% w/w, [acid] = 0.5 $mol.L^{-1}$, gelation bath: NaOH=10% i.e 2.5 $mol.L^{-1}$), the higher specific surface areas are obtained by using formic, acetic and maleic acids. It is supposed that the mesoporosity of hydrogels originates from the porosity between the neighboring chain fibrils [57]. Assuming that part of the microfibrillar structure is also found in lyophylizates, this result suggests that the use of acids also impact the structure of the dried forms. In this view, the entanglement density entrapped in the

hydrogel and chitosan- carboxylate interactions are likely to impact the mesoporous structure. In contrast to acetic and formic carboxylates, yielding stiff/extended chains in solutions, stiff fibrils in hydrogels and high BET surface due to the nanofibrillar structure, citric acid yielded lyophilizates with the lowest BET specific surface areas and thus the lowest porosities. At neutral pH, all acids in the hydrogels are mainly present in their fully dissociated carboxylate forms. The presence of carboxylates has been shown to induce ionic bonds with the chitosan chains [57]. During freeze-drying process these ionic bonds may also contribute to differences in the microstructure of the dried beads and hence to different BET specific surface areas.

According to **Table 4**, for the CS beads obtained by using acetic acid, the evolution of S_{BET} exhibits a maximum close to Cp = 4% w/w. The effect of the gelation bath composition was investigated for 4 samples: 2.5-AA-SQ / 3.5-AA-0.5 / 3.5-FA-0.5 / 3.5-CA-0.5. The use of EtOH as co-solvent both in the gelation baths and the storage solutions of the prills yielded to a significant increase in the S_{BET} values when using acetic and formic acids. On the contrary, the nature of the gelling bath only slightly affected the S_{BET} values of CS beads prepared from citric acid solutions. Again, the impact of the solvent composition is multifold. In particular, it has been shown that the presence of an alcohol in the solvent decreases the dielectric constant and changes the dissociation constant of the acid and the hydrophobic/hydrophilic interaction balance between chitosan chains [58] and chitosan-carboxylates interactions. In this work the samples gelled in hydroalcoholic NaOH solutions were further stored in hydroalcoholic solvent, thus EtOH not only modified the physicochemical conditions of gelation conditions but could also impact freeze-drying process, in particular the freezing step, which could explain the changes in S_{BET} results. Ethanol contained in the storage solution and hydrogel could influence cooling rate, nucleation rate and growth rate of ice crystals, with a global effect on the size of the crystals and resulting porous morphology (see SEM study below).

The comparison with the literature of the maximum values of S_{BET} attained in this work for the lyophilized CS beads (**Table 5**) indicates that a high specific surface area could be reached without any grafting or crosslinking of chitosan.

Therefore, assuming that all the samples display cylindrical shaped pores, the pore size distribution and average pore size diameters have been determined further by the Barrett-Joyner-Halenda (BJH) method. As expected for a freeze-drying process including the formation of a connected porous network after ice sublimation, all samples exhibit similar distributions with large mesopores (>40 nm) and few small mesopores (<10 nm), with total porous volumes ranging from 18 to 209 $cm^3.g^{-1}$ (**Table 4**). The beads prepared from chitosan and citric acid, display less meso-pores

than those prepared from other acids in the same conditions (see values of S_{BET} in **Table 5**). Such multiscale porous structure, with mesopores and macropores, was also observed by SEM (see section 3.2.2 below).

Table 4. Specific surface areas S_{BET} and pore volumes of the lyophilized beads prepared by varying the concentration of chitosan, the acid nature and the composition of the gellation bath. The samples labled with (*) were prepared through the use of ethanol in the gelling bath and the storage solution.

Cp % wt.	Acid – Concentation ($mol.L^{-1}$)	S_{BET} ($m^2.g^{-1}$)	V_{pores} ($cm^3.g^{-1}$)
2.5	Acetic – SQ	48	64
2.5	Acetic – SQ *	64	143
3.5	Acetic – 0.5	57	91
3.5	Acetic – 0.5 *	93	217
3.5	Formic – 0.5	57	84
3.5	Formic – 0.5 *	107	209
3.5	Citric – 0.5	46	72
3.5	Citric – 0.5 *	45	111
4	Acetic – 0.5	65	106
4	Formic – 0.5	61	98
4	Lactic – 0.5	42	83
4	Malic – 0.5	50	91
4	Maleic – 0.5	63	98
4	Citric – 0.5	12	18
4.5	Acetic – 0.75	60	92
5	Acetic – 0.75	42	86

SQ=Stoichiometric Quantity of protons to the number of amine groups (= 0.14 $mol.L^{-1}$ for 2.5% of CS and 0.2 $mol.L^{-1}$ for 3.5% of CS).

Table 5. Comparison of literature studies of the porous structure of chitosans-based materials obtained from different fabrication processes.

Material	S_{BET} ($m^2.g^{-1}$)	Source
Formaldehyde/CS spheres supercritical CO_2 dried	973	[59]
PEO/CS fibers	218	[60]
PEO/CS xerogels	0.103	[38]
Ni^{2+} imprinted CS resin	3.4	[61]
Cu^{2+} imprinted CS/sargassum	11.6	[62]
CS/PVA/TEOS xerogels	0.5	[63]
CS spheres supercritical CO_2 dried	111	[64]
CS spheres aerogels supercritical CO_2 dried	330	[65]

CS scaffolds supercritical CO_2 dried	135	[66]
CS prilled beads N_2 lyophilized	107	This work

3.2.2 Morphology - Scanning Electron Microscopy

The freeze-dried beads have almost kept the spherical shape of the parent hydrogel beads. Digital pictures of all samples were almost similar at millimeter scale and displayed more or less regular spheres of diameter ranging from 1.5 to 2 mm. As for example, **Fig. 9a and 9d** present the freeze-dried beads obtained from hydrogels gelated in NaOH aqueous bath, respectively without or with addition of EtOH (sample 3.5-FA-0.5). The microstructure differences between these freeze-dried beads are clearly evidenced on SEM images (**Fig. 9bc vs 9ef**). The sample gelated in NaOH aqueous solution displays an internal alveolar structure with large macropores, resembling a radial capillary structure, as previously observed by Sereni *et al*. [54] whereas the system gelated in the presence of EtOH presents a finer structure with smaller macropores. This fine texture confers the latter sample a higher specific surface area (107 vs 57 $m^2.g^{-1}$, **Table 4**). As explained above, this difference could be due to the changes in the gelation and freezing process of the hydrogels containing EtOH in liquid nitrogen. Thanks to the use of EtOH as a co-solvent in the gelling bath, a finer precipitated structure is better preserved. At the micron scale no systematic impact of the chitosan concentration or acid nature could be shown, even for the samples obtained from chitosan citrate which displayed specific rheological behavior and different porosities.

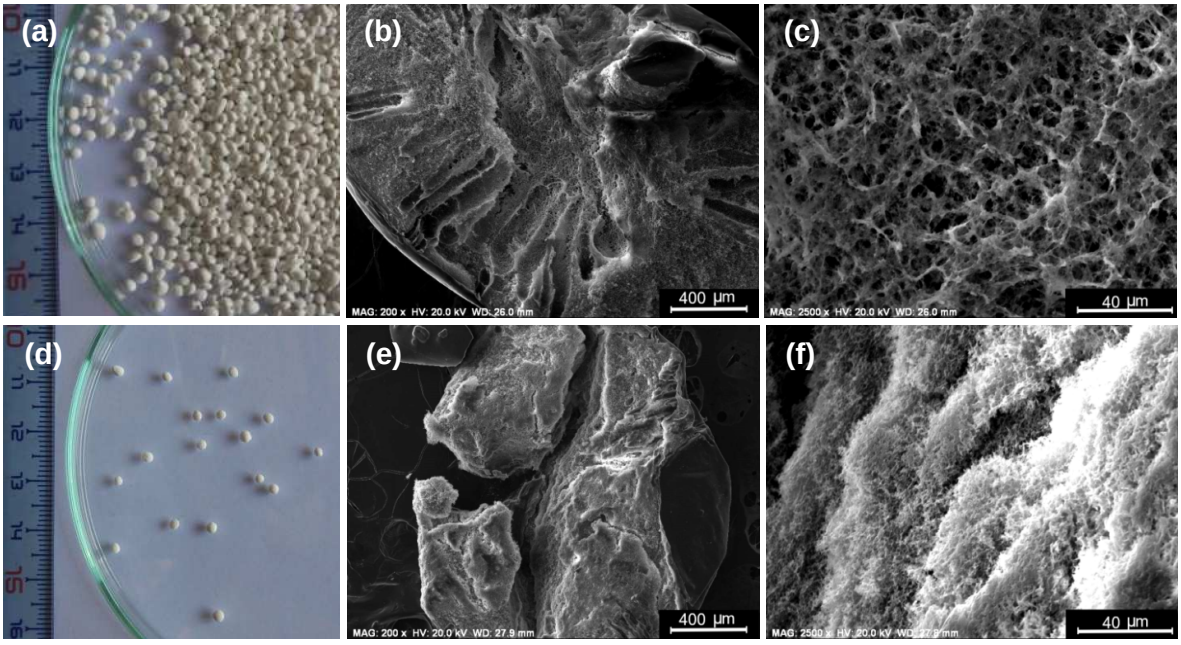

Fig. 9. Digital and SEM images of samples prepared from chitosan solution (Cp= 3.5% w/w in 0.5 mol.L^{-1} formic acid), gelated in NaOH aqueous solution (**a, b, c**) or by adding Ethanol as a co-solvent in the gelling bath (**d, e, f**). Ethanol induces the formation of a finer mesoporous structure.

3.2.3 Water uptake study

The effects of acid nature, chitosan concentration and gelling bath composition were also investigated upon the water adsorption of the prilled lyophilized beads. Varying the acid nature or chitosan concentration led to kinetic curves of similar profile. As an example, **Fig. 10** depicts the water adsorption kinetics of beads obtained from solutions prepared in different acids (at Cp=4%w/w with a constant acid concentration of 0.5 mol.L^{-1}). The adsorption uptakes varied from 203 to 269 mg.g^{-1} depending on the experimental conditions used to prepare the CS solutions, thus, rehydration in humid atmosphere (98% R.H.) was only partial in comparison with the pristine hydrogels containing more than 95% w/w of water. Nevertheless, the required time to achieve rehydration equilibrium clearly depends on the adsorption capacity. About 5h are required to achieve the equilibrium for the lowest water uptakes and about 7h for the highest ones.

Unexpectedly, the adsorption uptakes could not be correlated with the specific surface area (or the porous volume) values as the highest uptake (*i.e.*, 269 mg.g^{-1}) was reached for the material prepared by using citric acid for the dissolution of CS, having the lowest S_{BET} (12 $m^2.g^{-1}$) and lowest porous volume (Vp = 18 $cm^3.g^{-1}$) of the seven studied samples (**Table 4**). The lowest adsorption capacity was obtained for the sample prepared from lactic acid solution (i.e., 203 mg.g^{-1}), having a S_{BET} of 42 $m^2.g^{-1}$. In fact, the water adsorption uptake could result from remaining carboxylates interacting with chitosan in the hydrogel. When chitosan chains are neutralized in hydrogels, citric acid may develop strong interactions with chitosan via H-bonds and ionic bonds implying their hydroxyl and carboxylate groups. This probably contributes to the increases of hydrophilicity of the chains in the dry forms. Such interactions also decreases the crystalinity ratio which is known to increase water sorption in polymer matrices [67]. The general trends observed here concerning the water adsorption uptake is that the triacid induces higher adsorption than diacids, which themselves induce a higher adsorption than monoacids. Accordingly, the hydrophilicity of the lyophilized hydrogels slightly increased with the decrease of the first pKa of the acid used for the solubilization of chitosan: using different acids to solubilize chitosan offers a complexation partner with different physico-chemical properties, and thus yields beads with chitosan chains in different configurations and differently protonated/complexed according to the nature of the acid used.

Thus, each lyophilized material retains the typical physico-chemical signature of the acid used for its solubilization. The presence in the dried lyophilisates of protonated $-NH_3^+$ groups and dissociated carboxylate counterions could contribute to increase their hydrophilic character. Anions developping strong interactions with chitosan, like citric acid [68], may thus impose a stronger molecular signature within lyophilized forms.

Varying chitosan concentration from Cp= 3% to 4% in the acetate solutions was followed by an increase in the water adsorption capacity from 226 to 252 $mg.g^{-1}$ respectively. Thus, although the concentration of chitosan has very strong impact regarding the prillability, the influence of this parameter on the water uptake appears less important than that of the nature of the acid. Moreover, the presence of EtOH in the gelling bath was not found to have any significant influence on the water adsorption uptake, although the mesoporosity was strongly impacted.

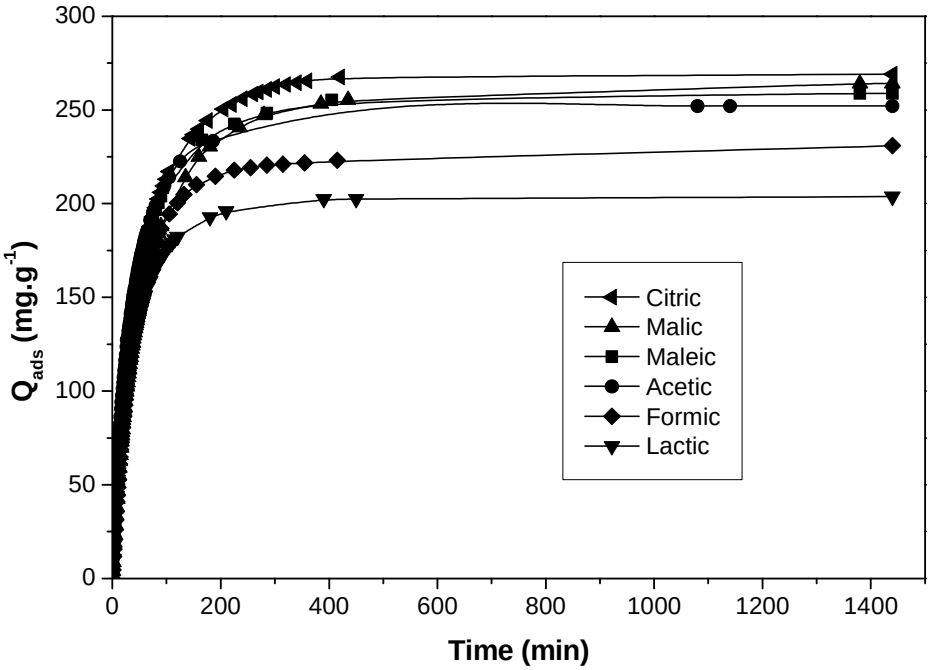

Fig. 10. Kinetics of the water vapor uptake at a 98% relative humidity on the lyophilized beads: effect of the nature of acid (acetic, formic, malic, lactic, citric and maleic) used to solubilize chitosan. The initial chitosan solutions used from sample preparation were concentrated at Cp=4%w/w with acid concentration of 0.5 $mol.L^{-1}$. Solid lines are gides for the eye.

4 Conclusion

The solubilization of chitosan in different organic acids (mono-, di- and tri-acids) has shown that the nature and concentration of the acid as well as the chitosan concentration has a great effect on the Newtonian viscosities of the solutions. This could be explained through the formation of carboxylic acid/chitosan/proton complexes that are favored in the case of polyacids (maleic and citric acids). The formation of these complexes probably acts on the density of charge of the polymer and thus decreases the viscosity of acidic chitosan solutions. On the opposite, acetic, formic, lactic and malic acids have led to the solutions with the highest viscosities.

Hydrogel beads of chitosan hydrogels of diameter ~2 mm have been prepared with the laminar jet break-up process, using solutions exibiting the optimized Newtonian viscosities (i.e. between 1 and 3 Pa.s). The storage moduli of these hydrogels were also dependent on the composition of the gelling bath. An initial solution of high viscosity generally has resulted in a final hydrogel with a high elasticity shear modulus, showing that the strength of the interchains interactions (entanglemements) in the gels may be inherited from the pristine solution. Spherical beads with acceptable mechanical properties obtained by the prilling process correspond to hydrogels with storage modulus G' > 3 kPa.s.

Freeze dried beads have exhibited large mesopores (>40 nm) and the main parameter to get a high S_{BET} was determined to be the compositon of the gelation bath. The beads gelled in NaOH (10% w/w) - EtOH (50% w/w) aqueous solutions from acetic acid or formic acid solution have shown the highest S_{BET} (up to 107 $m^2.g^{-1}$). As using citric acid in the pristine solution, the specific surface areas of the beads remained low and unchanged whatever the composition of the gelling bath.

The SEM images have revealed an alveolar porosity in absence of EtOH in the gelation bath whereas a more fibrous structure with smaller cavities was observed in the presence of EtOH, confirming the differences in the S_{BET} values. Thus, the use of EtOH allows to preserve the fine structure of the hydrogels prepared from chitosan acetate and formiate, although further improvements of the S_{BET} values could be obtained by CO_2 supercritical drying.

The water adsorption capacities of the freeze-dried beads did not depend on the S_{BET} values, but could be related to the nature of the acid used in the precursor solution, as the highest adsorption (269 $mg.g^{-1}$) was obtained for the beads from citric acid solutions (tri-acid). The trends of the vapor water uptake versus acid nature is citric > malic > maleic > acetic > formic > lactic acid, in relation with the acid strength and possible anion/chitosan interaction strengths.

For the envisioned application, formic acid is considered to be the best acid to solubilize chitosan, allowing an easy prilling process, yielding to beads having high mechanical strength and interesting porosity. Yet, solutions and lyophilizates prepared from citric acid solution have shown unusual

rheological behavior in comparison with monocarboxylic acids and the best water uptake, which makes it highly conceivable for acid mixes optimizations and other applications as rehydratable scaffolds for the biomedical field.

Funding

Funding for this project was provided by a grant (n°16-008947-01) from La Région-Auvergne-Rhône-Alpes.

References

[1] P. Pochanavanich, W. Suntornsuk, Fungal chitosan production and its characterization, Lett. Appl. Microbiol. 35 (2002) 17–21. https://doi.org/10.1046/j.1472-765X.2002.01118.x

[2] S.A. White, P.R. Farina, I. Fulton, Production and isolation of chitosan from Mucor rouxii., Appl. Environ. Microbiol. 38 (1979) 323–328.

[3] A. Fiamingo, J.A. de M. Delezuk, S. Trombotto, L. David, S.P. Campana-Filho, Extensively deacetylated high molecular weight chitosan from the multistep ultrasound-assisted deacetylation of beta-chitin, Ultrason. Sonochem. 32 (2016) 79–85. doi:10.1016/j.ultsonch.2016.02.021.

[4] K. Kurita, T. Sannan, Y. Iwakura, Studies on chitin, 4. Evidence for formation of block and random copolymers of N-acetyl-D-glucosamine and D-glucosamine by hetero-and homogeneous hydrolyses, Makromol. Chem. 178 (1977) 3197–3202. https://doi.org/10.1002/macp.1977.021781203

[5] G. Lamarque, M. Cretenet, C. Viton, A. Domard, New Route of Deacetylation of α- and β-Chitins by Means of Freeze−Pump Out−Thaw Cycles, Biomacromolecules. 6 (2005) 1380–1388. doi:10.1021/bm049322b.

[6] P. Sorlier, A. Denuzière, C. Viton, A. Domard, Relation between the degree of acetylation and the electrostatic properties of chitin and chitosan, Biomacromolecules. 2 (2001) 765–772. DOI: 10.1021/bm015531+

[7] A.R. Crofton, S.M. Hudson, K. Howard, T. Pender, A. Abdelgawad, D. Wolski, W.M. Kirsch, Formulation and characterization of a plasma sterilized, pharmaceutical grade chitosan powder, Carbohydr. Polym. 146 (2016) 420–426. doi:10.1016/j.carbpol.2016.03.003.

[8] J. Chedly, S. Soares, A. Montembault, Y. von Boxberg, M. Veron-Ravaille, C. Mouffle, M.-N. Benassy, J. Taxi, L. David, F. Nothias, Physical chitosan microhydrogels as scaffolds for spinal cord injury restoration and axon regeneration, Biomaterials. 138 (2017) 91–107. doi:10.1016/j.biomaterials.2017.05.024.

[9] M. Desorme, A. Montembault, J.-M. Lucas, C. Rochas, T. Bouet, L. David, Spinning of hydroalcoholic chitosan solutions, Carbohydr. Polym. 98 (2013) 50–63. doi:10.1016/j.carbpol.2013.04.070.

[10] A. Fiamingo, A. Montembault, S.-E. Boitard, H. Naemetalla, O. Agbulut, T. Delair, S.P. Campana-Filho, P. Menasché, L. David, Chitosan Hydrogels for the Regeneration of Infarcted Myocardium: Preparation, Physicochemical Characterization, and Biological Evaluation, Biomacromolecules. 17 (2016) 1662–1672. doi:10.1021/acs.biomac.6b00075.

[11] B.F. Bergel, L.M. da Luz, R.M.C. Santana, Comparative study of the influence of chitosan as coating of thermoplastic starch foam from potato, cassava and corn starch, Prog. Org. Coat. 106 (2017) 27–32. doi:10.1016/j.porgcoat.2017.02.010.

[12] M. Kaya, L. Česonienė, R. Daubaras, D. Leskauskaitė, D. Zabulionė, Chitosan coating of red kiwifruit (Actinidia melanandra) for extending of the shelf life, Int. J. Biol. Macromol. 85 (2016) 355–360. doi:10.1016/j.ijbiomac.2016.01.012.

[13] M. del R. Moreira, M. Pereda, N.E. Marcovich, S.I. Roura, Antimicrobial Effectiveness of Bioactive Packaging Materials from Edible Chitosan and Casein Polymers: Assessment on Carrot, Cheese, and Salami, J. Food Sci. 76 (2011) M54–M63. doi:10.1111/j.1750-3841.2010.01910.x.

[14] H. Altaher, The use of chitosan as a coagulant in the pre-treatment of turbid sea water, J. Hazard. Mater. 233–234 (2012) 97–102. doi:10.1016/j.jhazmat.2012.06.061.

[15] L. Dambies, E. Guibal, A. Roze, Arsenic(V) sorption on molybdate-impregnated chitosan beads, Colloids Surf. Physicochem. Eng. Asp. 170 (2000) 19–31. doi:10.1016/S0927-7757(00)00484-2.
[16] F. Quignard, A. Choplin, A. Domard, Chitosan: A Natural Polymeric Support of Catalysts for the Synthesis of Fine Chemicals, Langmuir. 16 (2000) 9106–9108. doi:10.1021/la000937d.
[17] I.C. Libio, R. Demori, M.F. Ferrão, M.I.Z. Lionzo, N.P. da Silveira, Films based on neutralized chitosan citrate as innovative composition for cosmetic application, Mater. Sci. Eng. C. 67 (2016) 115–124. doi:10.1016/j.msec.2016.05.009.
[18] E. Guibal, Interactions of metal ions with chitosan-based sorbents: a review, Sep. Purif. Technol. 38 (2004) 43–74. doi:10.1016/j.seppur.2003.10.004.
[19] J. Cao, H. Cao, Y. Zhu, S. Wang, D. Qian, G. Chen, M. Sun, W. Huang, Rapid and Effective Removal of Cu2+ from Aqueous Solution Using Novel Chitosan and Laponite-Based Nanocomposite as Adsorbent, Polymers. 9 (2016) 5. doi:10.3390/polym9010005.
[20] P.O. Osifo, H.W.J.. Neomagus, H. van der Merwe, D.J. Branken, Transport properties of chitosan membranes for zinc (II) removal from aqueous systems, Sep. Purif. Technol. 179 (2017) 428–437. doi:10.1016/j.seppur.2017.02.030.
[21] B. Liao, W. Sun, N. Guo, S. Ding, S. Su, Equilibriums and kinetics studies for adsorption of Ni(II) ion on chitosan and its triethylenetetramine derivative, Colloids Surf. Physicochem. Eng. Asp. 501 (2016) 32–41. doi:10.1016/j.colsurfa.2016.04.043.
[22] E. Elhefian, Chitosan Physical Forms: A Short Review, 2011.
[23] A. Djelad, A. Morsli, M. Robitzer, A. Bengueddach, F. di Renzo, F. Quignard, Sorption of Cu(II) Ions on Chitosan-Zeolite X Composites: Impact of Gelling and Drying Conditions, Molecules. 21 (2016) 109. doi:10.3390/molecules21010109.
[24] A. Primo, F. Quignard, Chitosan as efficient porous support for dispersion of highly active gold nanoparticles: design of hybrid catalyst for carbon–carbon bond formation, Chem. Commun. 46 (2010) 5593. doi:10.1039/c0cc01137a.
[25] C. Peniche, W. Argüelles-Monal, H. Peniche, N. Acosta, Chitosan: An Attractive Biocompatible Polymer for Microencapsulation, 2003. doi:10.1002/mabi.200300019.
[26] N. Arya, S. Chakraborty, N. Dube, D.S. Katti, Electrospraying: A facile technique for synthesis of chitosan-based micro/nanospheres for drug delivery applications, J. Biomed. Mater. Res. B Appl. Biomater. 88B (2009) 17–31. doi:10.1002/jbm.b.31085.
[27] X. Wang, T. Nakamoto, I. Dulińska-Molak, N. Kawazoe, G. Chen, Regulating the stemness of mesenchymal stem cells by tuning micropattern features, J. Mater. Chem. B. 4 (2016) 37–45. doi:10.1039/C5TB02215K.
[28] G. Auriemma, T. Mencherini, P. Russo, M. Stigliani, R.P. Aquino, P. Del Gaudio, Prilling for the development of multi-particulate colon drug delivery systems: Pectin vs. pectin–alginate beads, Carbohydr. Polym. 92 (2013) 367–373. doi:10.1016/j.carbpol.2012.09.056.
[29] F. Séquier, V. Faivre, G. Daste, M. Renouard, S. Lesieur, Critical parameters involved in producing microspheres by prilling of molten lipids: From theoretical prediction of particle size to practice, Eur. J. Pharm. Biopharm. 87 (2014) 530–540. doi:10.1016/j.ejpb.2014.03.005.
[30] P. Del Gaudio, G. Auriemma, P. Russo, T. Mencherini, P. Campiglia, M. Stigliani, R.P. Aquino, Novel co-axial prilling technique for the development of core–shell particles as delayed drug delivery systems, Eur. J. Pharm. Biopharm. 87 (2014) 541–547. doi:10.1016/j.ejpb.2014.02.010.
[31] Z.-H. Zhang, Z. Han, X.-A. Zeng, X.-Y. Xiong, Y.-J. Liu, Enhancing mechanical properties of chitosan films via modification with vanillin, Int. J. Biol. Macromol. 81 (2015) 638–643. doi:10.1016/j.ijbiomac.2015.08.042.
[32] S. Hirano, C. Itakura, H. Seino, Y. Akiyama, I. Nonaka, N. Kanbara, T. Kawakami, Chitosan as an ingredient for domestic animal feeds, J. Agric. Food Chem. 38 (1990) 1214–1217. DOI: 10.1021/jf00095a012
[33] H.G. Preuss, G.R. Kaats, Chitosan as a Dietary Supplement for Weight Loss: A Review, (n.d.) 17. DOI: 10.1021/jf00095a012
[34] M. Sumiyoshi, Y. Kimura, Low molecular weight chitosan inhibits obesity induced by feeding a high-fat diet long-term in mice, J. Pharm. Pharmacol. 58 (2006) 201–207. doi:10.1211/jpp.58.2.0007.
[35] A. Hirai, H. Odani, A. Nakajima, Determination of degree of deacetylation of chitosan by 1H NMR spectroscopy, Polym. Bull. 26 (1991) 87–94.
[36] F. Brunel, L. Véron, C. Ladavière, L. David, A. Domard, T. Delair, Synthesis and structural characterization of chitosan nanogels, Langmuir. 25 (2009) 8935–8943. doi:10.1021/la9002753.
[37] C. Schatz, C. Viton, T. Delair, C. Pichot, A. Domard, Typical Physicochemical Behaviors of Chitosan in Aqueous Solution, Biomacromolecules. 4 (2003) 641–648. doi:10.1021/bm025724c.

[38] L. Martinez, F. Agnely, R. Bettini, M. Besnard, P. Colombo, G. Couarraze, Preparation and characterization of chitosan based micro networks: Transposition to a prilling process, J. Appl. Polym. Sci. 93 (2004) 2550–2558. doi:10.1002/app.20785.
[39] C. Heinzen, I. Marison, A. Berger, U. von Stockar, Use of vibration technology for jet break-up for encapsulation of cells, microbes and liquids in monodisperse microcapsules, Landbauforsch. Völkenrode SH241. (2002) 19–25.
[40] A.B. García-Bermejo, A. Cardelle-Cobas, A.I. Ruiz-Matute, F. Montañés, A. Olano, N. Corzo, Effect of drying methods on the reactivity of chitosan towards Maillard reaction, Food Hydrocoll. 29 (2012) 27–34. doi:10.1016/j.foodhyd.2012.01.014.
[41] S. Brunauer, P.H. Emmett, E. Teller, Adsorption of Gases in Multimolecular Layers, J. Am. Chem. Soc. 60 (1938) 309–319. doi:10.1021/ja01269a023.
[42] E.P. Barrett, L.G. Joyner, P.P. Halenda, The determination of pore volume and area distributions in porous substances. I. Computations from nitrogen isotherms, J. Am. Chem. Soc. 73 (1951) 373–380. DOI: 10.1021/ja01145a126
[43] N. Calero, J. Muñoz, P. Ramírez, A. Guerrero, Flow behaviour, linear viscoelasticity and surface properties of chitosan aqueous solutions, Food Hydrocoll. 24 (2010) 659–666. doi:10.1016/j.foodhyd.2010.03.009.
[44] M. Hamdine, M.-C. Heuzey, A. Bégin, Effect of organic and inorganic acids on concentrated chitosan solutions and gels, Int. J. Biol. Macromol. 37 (2005) 134–142. doi:10.1016/j.ijbiomac.2005.09.009.
[45] A. Montembault, C. Viton, A. Domard, Rheometric Study of the Gelation of Chitosan in Aqueous Solution without Cross-Linking Agent, Biomacromolecules. 6 (2005) 653–662. doi:10.1021/bm049593m.
[46] M. Mucha, Rheological characteristics of semi-dilute chitosan solutions, Macromol. Chem. Phys. 198 (1997) 471–484. doi:10.1002/macp.1997.021980220.
[47] C. Halimi, A. Montembault, A. Guerry, T. Delair, E. Viguier, R. Fulchiron, L. David, Chitosan solutions as injectable systems for dermal filler applications: Rheological characterization and biological evidence, in: IEEE, 2015: pp. 2596–2599. doi:10.1109/EMBC.2015.7318923.
[48] CRC Handbook of Chemistry and Physics, 2009−2010, 90th ed., J. Am. Chem. Soc. 131 (2009) 12862–12862. doi:10.1021/ja906434c.
[49] D. Filion, M. Lavertu, M.D. Buschmann, Ionization and Solubility of Chitosan Solutions Related to Thermosensitive Chitosan/Glycerol-Phosphate Systems, Biomacromolecules. 8 (2007) 3224–3234. doi:10.1021/bm700520m.
[50] pH Calculation and Acid-Base Titration Curves - Freeware for Data Analysis and Simulation, (n.d.). http://www.iq.usp.br/gutz/Curtipot_.html (accessed September 26, 2018).
[51] M.V. Shamov, S.Y. Bratskaya, V.A. Avramenko, Interaction of Carboxylic Acids with Chitosan: Effect of pK and Hydrocarbon Chain Length, J. Colloid Interface Sci. 249 (2002) 316–321. doi:10.1006/jcis.2002.8248.
[52] S. Cataldo, C. De Stefano, A. Gianguzza, D. Piazzese, S. Sammartano, Speciation of chitosan with low and high molecular weight carboxylates in aqueous solution, Chem. Speciat. Bioavailab. 21 (2009) 81–91. doi:10.3184/095422909X449418.
[53] L. Rami, S. Malaise, S. Delmond, J.-C. Fricain, R. Siadous, S. Schlaubitz, E. Laurichesse, J. Amédée, A. Montembault, L. David, L. Bordenave, Physicochemical modulation of chitosan-based hydrogels induces different biological responses: Interest for tissue engineering: In vitro and in vivo behaviour of chitosan hydrogels with tuneable properties, J. Biomed. Mater. Res. A. 102 (2014) 3666–3676. doi:10.1002/jbm.a.35035.
[54] N. Sereni, A. Enache, G. Sudre, A. Montembault, C. Rochas, P. Durand, M.-H. Perrard, G. Bozga, J.-P. Puaux, T. Delair, L. David, Dynamic structuration of physical chitoan hydrogels, Langmuir. (2017). doi:10.1021/acs.langmuir.7b02997.
[55] C. Pochat-Bohatier, V. Antoine, B. Denis, V. Laurent, D. Laurent, F. Catherine, Development and characterization of composite chitosan/active carbon hydrogels for a medical application, J. Appl. Polym. Sci. 128 (2013) 2945–2953. doi:10.1002/app.38414.
[56] J. Tanigawa, N. Miyoshi, K. Sakurai, Characterization of chitosan/citrate and chitosan/acetate films and applications for wound healing, J. Appl. Polym. Sci. 110 (2008) 608–615. doi:10.1002/app.28688.
[57] T. Furuike, D. Komoto, H. Hashimoto, H. Tamura, Preparation of chitosan hydrogel and its solubility in organic acids, Int. J. Biol. Macromol. 104 (2017) 1620–1625. doi:10.1016/j.ijbiomac.2017.02.099.

[58] M. Robitzer, L. David, C. Rochas, F.D. Renzo, F. Quignard, Nanostructure of Calcium Alginate Aerogels Obtained from Multistep Solvent Exchange Route, Langmuir. 24 (2008) 12547–12552. doi:10.1021/la802103t.
[59] A. Montembault, C. Viton, A. Domard, Rheometric study of the gelation of chitosan in a hydroalcoholic medium, Biomaterials. 26 (2005) 1633–1643. doi:10.1016/j.biomaterials.2004.06.029.
[60] S. Zhang, J. Feng, J. Feng, Y. Jiang, Formation of enhanced gelatum using ethanol/water binary medium for fabricating chitosan aerogels with high specific surface area, Chem. Eng. J. 309 (2017) 700–707. doi:10.1016/j.cej.2016.10.098.
[61] M.I. Shariful, S.B. Sharif, J.J.L. Lee, U. Habiba, B.C. Ang, M.A. Amalina, Adsorption of divalent heavy metal ion by mesoporous-high surface area chitosan/poly (ethylene oxide) nanofibrous membrane, Carbohydr. Polym. 157 (2017) 57–64. doi:10.1016/j.carbpol.2016.09.063.
[62] T. Tianwei, H. Xiaojing, D. Weixia, Adsorption behaviour of metal ions on imprinted chitosan resin, J. Chem. Technol. Biotechnol. 76 (2001) 191–195. doi:10.1002/jctb.358.
[63] H. Liu, F. Yang, Y. Zheng, J. Kang, J. Qu, J.P. Chen, Improvement of metal adsorption onto chitosan/Sargassum sp. composite sorbent by an innovative ion-imprint technology, Water Res. 45 (2011) 145–154. doi:10.1016/j.watres.2010.08.017.
[64] M.A. Kamal, T. Yasin, L. Reinert, L. Duclaux, Adsorptive removal of copper (II) ions from aqueous solution by silane cross-linked chitosan/PVA/TEOS beads: kinetics and isotherms, Desalination Water Treat. 57 (2016) 4037–4048. doi:10.1080/19443994.2014.991761.
[65] M. Díez-Municio, A. Montilla, M. Herrero, A. Olano, E. Ibáñez, Supercritical CO2 impregnation of lactulose on chitosan: A comparison between scaffolds and microspheres form, J. Supercrit. Fluids. 57 (2011) 73–79. doi:10.1016/j.supflu.2011.02.001.
[66] F. Quignard, R. Valentin, F. Di Renzo, Aerogel materials from marine polysaccharides, New J. Chem. 32 (2008) 1300. doi:10.1039/b808218a.
[67] K. Rinki, P.K. Dutta, Chitosan Based Scaffolds by Lyophilization and sc.CO_2 Assisted Methods for Tissue Engineering Applications, J. Macromol. Sci. Part A. 47 (2010) 429–434. doi:10.1080/10601321003659630.
[68] L. Valentine, Studies on the sorption of moisture by polymers. I. Effect of crystallinity, J. Polym. Sci. 27 (1958) 313–333. doi:10.1002/pol.1958.1202711526.
[69] X. Shu, Novel pH-sensitive citrate cross-linked chitosan film for drug controlled release, Int. J. Pharm. 212 (2001) 19–28. doi:10.1016/S0378-5173(00)00582-2.